

Performance, structure, and stability of SiC/Al multilayer films for extreme ultraviolet applications

David L. Windt* and Jeffrey A. Bellotti

Reflective X-ray Optics LLC, 1361 Amsterdam Avenue, Suite 3B, New York, New York 10027, USA

*Corresponding author: davidwindt@gmail.com

Received 14 July 2009; accepted 8 August 2009;
posted 14 August 2009 (Doc. ID 114261); published 1 September 2009

We report on the performance, structure and stability of periodic multilayer films containing silicon carbide (SiC) and aluminum (Al) layers designed for use as reflective coatings in the extreme ultraviolet (EUV). We find that SiC/Al multilayers prepared by magnetron sputtering have low stress, good temporal and thermal stability, and provide good performance in the EUV, particularly for applications requiring a narrow spectral bandpass, such as monochromatic solar imaging. Transmission electron microscopy reveals amorphous SiC layers and polycrystalline Al layers having a strong $\langle 111 \rangle$ texture, and relatively large roughness associated with the Al crystallites. Fits to EUV reflectance measurements also indicate large interface widths, consistent with the electron microscopy results. SiC/Al multilayers deposited by reactive sputtering with nitrogen comprise Al layers that are nearly amorphous and considerably smoother than films deposited nonreactively, but no improvements in EUV reflectance were obtained. © 2009 Optical Society of America

OCIS codes: 230.4170, 310.1620, 310.6860, 340.0340, 350.1260.

1. Introduction

Nanometer-scale multilayer films designed for use as normal-incidence reflectors in the extreme ultraviolet (EUV) are now widely used for a variety of applications in science and industry. For some of these applications the narrow spectral response intrinsic to periodic multilayers is exploited in order to filter the incident radiation upon reflection, so that the coatings also act, in effect, as efficient, reflective, bandpass filters. For example, the narrow spectral response of reflective EUV multilayers is essential to their use in imaging optics for solar physics, where these coatings can be deposited onto figured mirror substrates used to construct high-resolution telescopes for monochromatic imaging of the sun. The multilayer coatings for solar imaging are designed to provide high reflectance at a specific EUV wavelength that corresponds to emission from a particular

spectral line (or line complex) that originates from ionized atoms in the solar atmosphere; in order to avoid “spectral contamination” of the resultant image, the multilayer coatings must also have relatively low reflectance at nearby bright wavelengths, as we discuss in more detail below.

While there are by now several available multilayer material combinations that provide good performance in the EUV, there nevertheless remain large portions of the EUV spectral region where new or better multilayers are needed. For example, in solar physics applications, Si/Mo multilayers have been used successfully in a number of satellite instruments [1–3] over the past two decades to provide high reflectance in the wavelength range of $\lambda \sim 13\text{--}30\text{ nm}$. At the short wavelength end of this region, the performance of Si/Mo is essentially unsurpassed. However, at wavelengths longer than approximately 25 nm, the peak reflectance of Si/Mo is relatively low, and the spectral bandpass relatively high, owing principally to the large absorption of

0003-6935/09/264932-10\$15.00/0
© 2009 Optical Society of America

Si far from the Si L-edge near $\lambda = 12.4$ nm, and of Mo far from its M-edge near $\lambda = 6$ nm.

Because of the performance limitations of Si/Mo multilayers at longer EUV wavelengths, alternative coatings have been actively pursued in recent years. Promising new multilayer systems have thus emerged, such as SiC/Mg [3,4], Si/B₄C [5,6], and Si/SiC [6], that have been optimized for use in the wavelength range $\lambda \sim 25$ –35 nm. Unfortunately, the multilayers just listed all have some drawbacks that may limit their utility for many applications. Specifically, questions remain about the long-term stability of SiC/Mg, while Si/B₄C and Si/SiC both have very large film stress, which can lead to stress-driven adhesion failures and/or substrate distortions that can degrade optical performance. A number of new multilayer systems designed for even longer wavelengths have been developed as well in recent years, such as Si/Sc [7], Si/Gd [8], and others [9]. In spite of these advances, however, interest remains high in finding stable multilayers having low stress and improved EUV performance and stability.

Aluminum has long been an intriguing material for use in EUV multilayers in this wavelength range because of its very low absorption below the Al L-edge near 17 nm. A number of candidate material combinations containing Al have been proposed, such as Y/Al, Zr/Al, and Nb/Al, and these systems all show very promising theoretical performance in the EUV. Good EUV performance has been realized experimentally for Zr/Al multilayers [10], however, the temporal stability of this system is unknown. (Temporal stability is crucial for many applications, especially satellite instruments for solar physics that are intended to operate over a period of years, or even decades.) Y/Al multilayers have also been investigated experimentally, but the performance and stability of these coatings was found to be poor: as-deposited periodic Y/Al films were found to have only $\sim 18\%$ peak reflectance near $\lambda \sim 19$ nm, significantly less than that expected theoretically. Furthermore, these coatings degraded steadily, having peak reflectance below 1% after a period of ~ 300 days storage in air. The incorporation of 0.3-nm-thick carbon barrier layers at each interface in Y/Al multilayers increased the as-deposited reflectance to more than 40% near $\lambda \sim 19$ nm, but these films degraded rapidly as well, yielding only $\sim 22\%$ reflectance after ~ 300 days [11].

The SiC/Al system is another candidate multilayer coating containing aluminum that shows good theoretical performance in the EUV. The very narrow spectral response of this multilayer makes it especially attractive for applications such as solar imaging, for the reasons outlined above. For example, as compared to Si/Mo multilayers, SiC/Al coatings could provide comparable (or potentially higher) peak reflectance as Si/Mo at the Fe XV solar line at $\lambda = 28.4$ nm, yet the spectral bandpass of SiC/Al is much smaller than Si/Mo. Thus, a SiC/Al multilayer tuned to $\lambda = 28.4$ nm, or alternatively to the Fe XVI line at $\lambda = 33.5$ nm, would provide much lower reflectance than Si/Mo at the nearby, bright He II line ($\lambda = 30.4$ nm), as illustrated in Fig. 1(a). Telescope mirrors coated with SiC/Al rather than Si/Mo for a 28.4 nm (or 33.5 nm) wavelength would thus provide much more “spectrally pure” images, in that the 30.4 nm spectral contamination would be reduced considerably, as we discuss quantitatively below. Similarly, as illustrated in Fig. 1(b), SiC/Al coatings would also give much better spectral resolution at the Fe XII ($\lambda = 19.5$ nm) and Fe XIV ($\lambda = 21.1$ nm) lines relative to Si/Mo coatings, albeit with somewhat lower reflection efficiency.

The SiC/Al multilayer system was investigated experimentally for use as a reflective coating in the EUV as early as 1996 in Japan [12]. More recently, researchers in France have made significant progress in understanding the characteristics of these films [13]. SiC/Al multilayers have also been investigated recently for their promising mechanical properties as well [14].

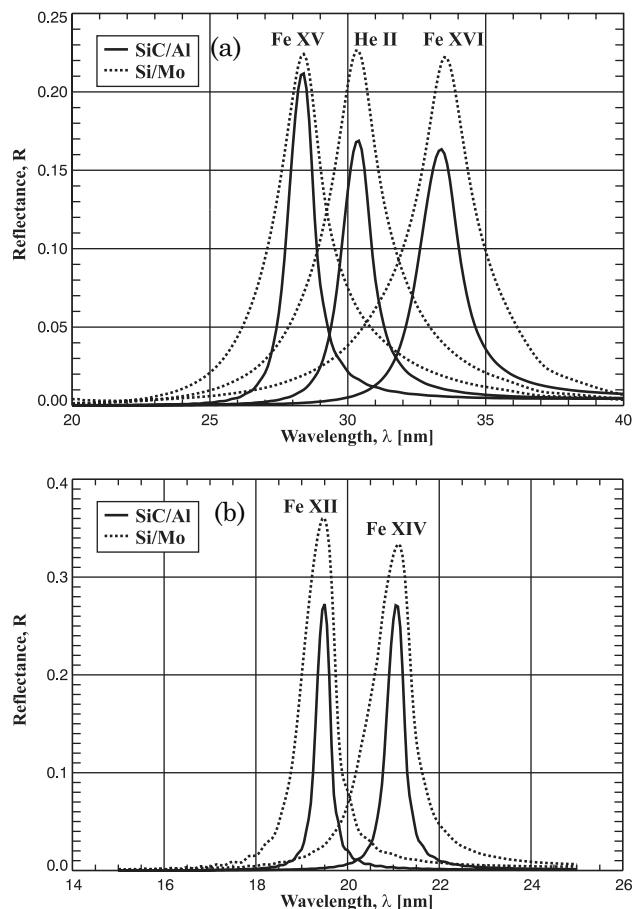


Fig. 1. Calculated reflectance of SiC/Al and Si/Mo multilayers optimized for narrow spectral response at (a) the Fe XV ($\lambda = 28.4$ nm), He II ($\lambda = 30.4$ nm), and Fe XVI ($\lambda = 33.5$ nm) solar emission lines; and (b) the Fe XII ($\lambda = 19.5$ nm) and Fe XIV ($\lambda = 21.1$ nm) lines. SiC/Al provides significantly greater spectral resolution. The interface widths used for these calculations are based on experimental results obtained from multilayers similar to those calculated here.

In this paper we report on the performance, structure, and stability of periodic SiC/Al multilayers designed for use as EUV reflectors in the range of $\lambda \sim 17\text{--}65\text{ nm}$. Our films were fabricated by magnetron sputtering, and we have employed a variety of characterization techniques to better understand the layer and interface structure, and also the temporal and thermal stability: in addition to normal-incidence EUV reflectometry, we have studied these films using x-ray reflectance (XRR), x-ray diffraction (XRD), high-resolution cross-sectional transmission electron microscopy (HRTEM), and wafer curvature to measure film stress as a function of temperature. In the sections that follow we describe our experimental techniques in detail, we present our results, and discuss our findings. We conclude with a summary and discussion of our most significant results.

2. Experimental Procedures

The multilayer films discussed here were prepared by DC magnetron sputtering using a deposition system that has been described previously [15]. Solid, rectangular targets of Al (99.999% purity) and SiC (99.0% purity), measuring $50\text{ cm} \times 9\text{ cm} \times 0.6\text{ cm}$, were used. The cathodes were operated in regulated power mode, with 400 W applied to each target. The sputter gas was Ar (99.999% purity), and the gas pressure was held constant at $1.60 \pm 0.01\text{ mTorr}$. (For certain samples, reactive sputtering with an Ar/N₂ gas mixture was used, as will be described in Section 3.) The vacuum chamber is cryopumped, and the background pressure in the chamber prior to deposition was in the range of $1\text{--}3 \times 10^{-7}\text{ Torr}$ in all cases.

Multilayer films were deposited onto 75 mm diameter, prime-grade Si (100) wafers. Individual Al and SiC layer thicknesses were adjusted by varying the computer-controlled rotation rate and hence the exposure time, of the substrate as it passes over each magnetron cathode. The effective deposition rates, computed using layer thicknesses determined from XRR measurements (described below) divided by the known exposure times, were found to be $\sim 0.06\text{ nm/s}$ for SiC, and $\sim 0.27\text{ nm/s}$ for Al.

XRR measurements were made in the $\theta\text{--}2\theta$ geometry using a four-circle x-ray diffractometer having a sealed-tube Cu source and a Ge (111) crystal monochromator tuned to the Cu K- α line ($\lambda = 0.154\text{ nm}$, $E = 8.04\text{ keV}$.) The angular resolution of this system is estimated to be $\delta\theta \sim 0.015^\circ$. Fits to the XRR data (performed using IMD [16]) were used to determine the multilayer period, with an estimated precision of $\delta d \sim \pm 0.01\text{ nm}$.

For selected samples, as described below, XRD measurements were performed by Evans Analytical Group LLC (EAG), Round Rock, Texas, in order to make quantitative measurements of both the in-plane and out-of-plane Al crystal sizes. For these measurements, a Rigaku Ultima III system equipped with an in-plane arm was used. A multilayer colli-

ating mirror was used to create a parallel incident beam of Cu K- α radiation.

Transmission electron microscopy of selected samples was performed by EAG, Sunnyvale, California. Cross-sectional samples were prepared by the wedge polishing technique and then ion milled to electron transparency using 3kV Ar⁺ ions and a Gatan Model 691 Precision Ion Polishing System. Measurements were made using a JEOL model 2010 microscope operating at 200 keV.

Film stress was measured using a Toho Technologies Flexus model 2320S wafer curvature system. The curvature of the Si wafer substrates (0.4 mm nominal thickness) was measured along two orthogonal directions before and after film deposition. The total film thickness as determined by XRR was used to compute film stress, following the standard formalism based on the Stoney equation [17]. In addition, stress-versus-temperature measurements, from room temperature (25 °C) to 300 °C, were made on selected multilayer samples using the same instrument.

EUV reflectance measurements were made near normal incidence (5°) as a function of wavelength using a laser-plasma-based reflectometer at Reflective X-ray Optics (RXO), also described previously [15]. The reflectance of selected samples was also measured using synchrotron radiation at 5° incidence, using the Naval Research Laboratory reflectometer on beamline X24C at the National Synchrotron Light Source (NSLS), Brookhaven National Laboratory, or at the Calibration and Standards beamline 6.3.2 at the Advanced Light Source (ALS) [18]. Fits to the EUV data (also made using IMD) were used to infer interface widths, using published optical constants, as described in Section 3.

3. Results and Discussion

In order to assess how the performance of periodic SiC/Al multilayers varies as a function of the relative thicknesses of the individual SiC and Al layers, we deposited and characterized a series of eight films for which the SiC fractional layer thickness, Γ_{SiC} , defined here as $\Gamma_{\text{SiC}} = d_{\text{SiC}}/(d_{\text{SiC}} + d_{\text{Al}}) = d_{\text{SiC}}/d$, was systematically varied over the range of $\Gamma_{\text{SiC}} = 0.2\text{--}0.5$. The multilayer period, d , was adjusted slightly in each case so that the peak reflectance occurred near $\lambda = 28.4\text{ nm}$; the multilayer period was thus $d \sim 15.2 \pm 0.2\text{ nm}$ and, for maximum reflectance in this wavelength range, a total of $N = 40$ bilayers were deposited in each case.

Shown in Fig. 2 are the normal-incidence reflectance versus wavelength measurements for these eight films, and in Fig. 3 we plot the peak reflectance and spectral bandpass (quantified in terms of the FWHM of the multilayer Bragg peak) determined from these measurements as a function of Γ_{SiC} . The reflectance measurements shown in Figs. 2 and 3 were made using the RXO reflectometer mentioned in Section 2. We also plot, as a function of Γ_{SiC} , in

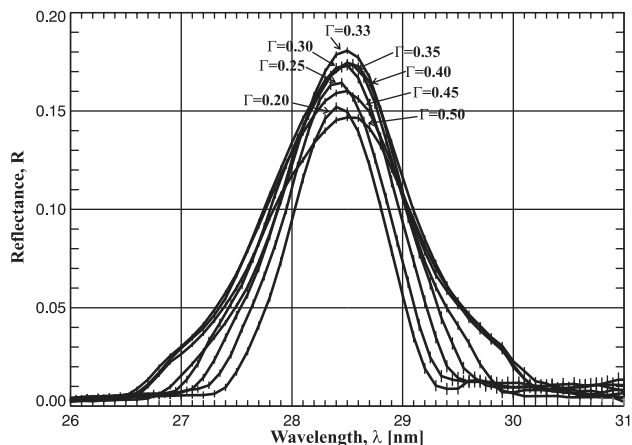


Fig. 2. Experimental reflectance versus wavelength for SiC/Al multilayers measured as a function of the SiC fractional layer thickness, Γ_{SiC} .

Fig. 3 the as-deposited film stress determined from wafer curvature.

As can be seen from Figs. 2 and 3, the peak reflectance varies slowly with Γ_{SiC} , ranging from $R_{\text{max}} = 14.7\text{--}18\%$, with the highest peak reflectance occurring for the case $\Gamma_{\text{SiC}} = 0.33$. The spectral bandpass increases monotonically with Γ_{SiC} , ranging from 1 to 1.6 nm FWHM over the range of $\Gamma_{\text{SiC}} = 0.2$ to 0.5. These trends agree with those expected from modeling, assuming the optical constants for Al and SiC from [19]. The as-deposited stresses were all com-

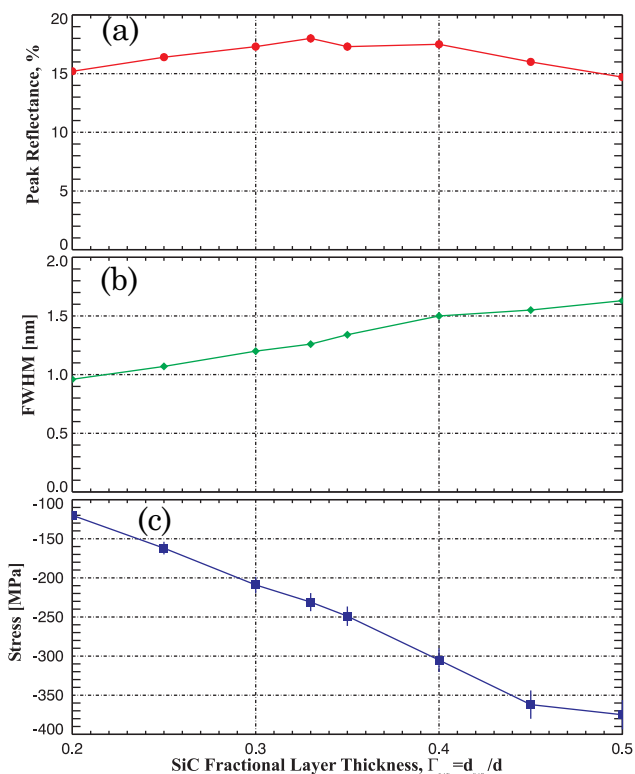


Fig. 3. (Color online) (a) Experimental peak reflectance, (b) spectral bandpass, and (c) film stress as functions of SiC fractional layer thickness, Γ_{SiC} , for the SiC/Al multilayers shown in Fig. 2.

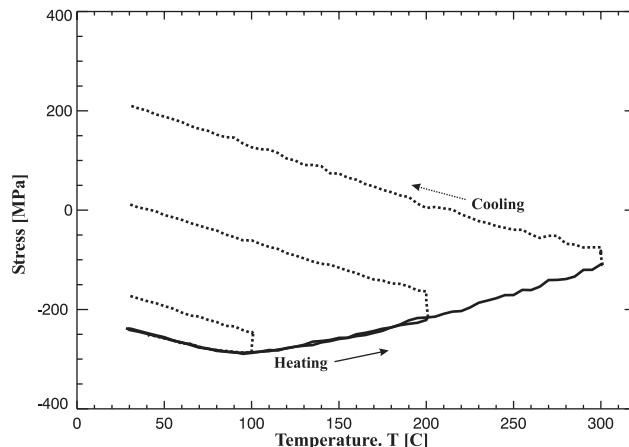


Fig. 4. Film stress measured as a function of temperature for SiC/Al multilayers having $d = 15.3$ nm, $N = 40$, and $\Gamma = 0.33$.

pressive and relatively small, increasing nearly linearly from -120 to -375 MPa over this same range of Γ values.

Based on the results shown in Figs. 2 and 3, we prepared three additional films tuned near $\lambda = 28.4$ nm having $\Gamma_{\text{SiC}} = 0.33$ for thermal annealing studies. Shown in Fig. 4 are the stress-versus-temperature measurements obtained with these films. For this experiment, the first sample was heated to 100°C (with N_2 gas flow over the film surface to prevent oxidation) at a rate of $5^\circ/\text{min}$, then held at 100°C for a period of 30 min, and finally allowed to cool to room temperature. The two remaining samples were heated (at the same rate) to 200°C and 300°C , respectively, held at temperature for 30 min, and allowed to cool to room temperature.

As can be seen from Fig. 4, the stress in the SiC/Al multilayer film heated to 100°C increases nearly linearly with temperature up to about 90°C , owing to the mismatch in thermal expansion coefficients between the film and substrate. Above 90°C the stress begins to relax. The stress decreases further while the sample is held at 100°C , and then, upon cooling, the stress decreases nearly linearly, again due to the thermal expansion coefficient mismatch. Subsequent heating/cooling cycles follow the same pattern, with further relaxation at temperatures above 90°C . Upon cooling to room temperature, the final stress in the sample heated to 300°C was in excess of 200 MPa tensile, an increase of more than 400 MPa.

Shown in Fig. 5 are the normal-incidence reflectance measurements of the annealed samples shown in Fig. 4. While there is no measurable change in reflectance after heating to 100°C , annealing to higher temperatures causes a significant drop in peak reflectance: the 200°C sample has peak reflectance of 17% (as compared to 18% for the as-deposited and 100°C films), while the film heated to 300°C has only 11% peak reflectance. There are no measurable changes in peak wavelength for the annealed samples; XRR measurements (not shown) of the samples shown in Figs. 4 and 5 indicate no measurable

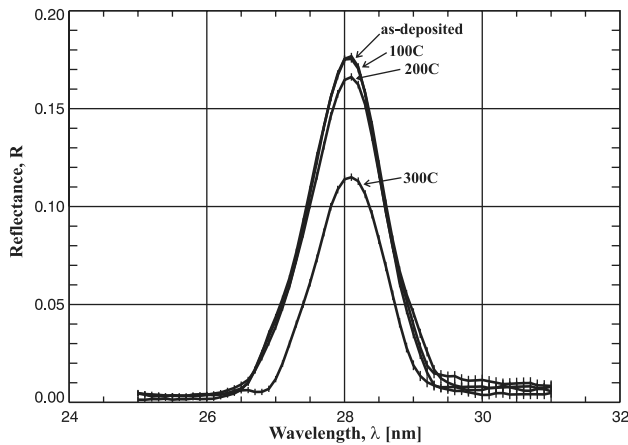


Fig. 5. Reflectance versus wavelength obtained on the annealed samples shown in Fig. 4.

changes in multilayer period, consistent with the EUV results.

To help identify any microstructural changes that may be associated with the changes in stress and EUV reflectance upon thermal annealing just described, we obtained HRTEM images of the as-deposited and 300 °C samples shown in Figs. 4 and 5. The HRTEM results are shown in Fig. 6. As can be seen in these images, in both films the SiC layers are amorphous, while the Al layers are polycrystalline, exhibiting a strong $\langle 111 \rangle$ texture (as determined from both selected-area electron diffraction (SAED)—not shown in Fig. 6—as well as XRD measurements.) Although there are no large, obvious mixed SiC–Al interlayers apparent in these images, as is typical of many other EUV multilayers, the crystallinity of the Al layers is apparently contributing significantly to the interfacial roughness. As we discuss in detail below, this interfacial roughness is likely to be the main limitation on EUV performance. In any case, qualitatively, the sample annealed at 300 °C

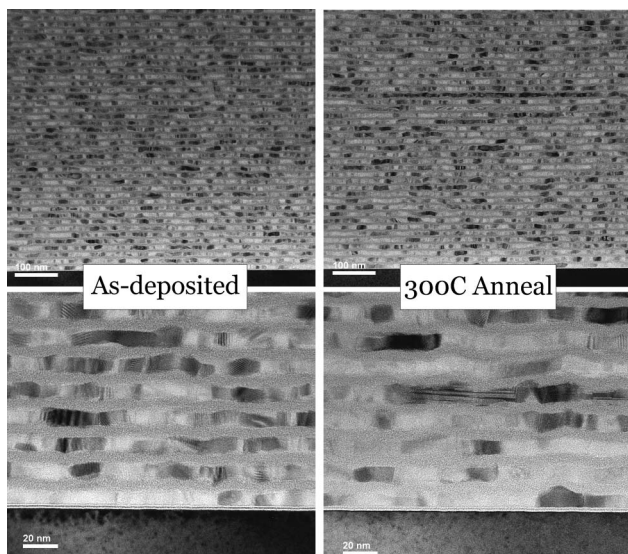


Fig. 6. HRTEM images of the as-deposited (left) and 300 C (right) annealed sample shown in Figs. 4 and 5.

looks remarkably similar to the as-deposited film, with no large, obvious changes in SiC or Al layer thicknesses, or in interface structure.

Quantitative measurements of the Al grain size of the films shown in Fig. 6, both in-plane and out-of-plane (i.e., along the growth direction), were determined from XRD analysis by measuring the widths of the (220) and (111) reflections, respectively. We find that the in-plane grain size increased considerably upon thermal annealing to 300 °C, from 15.8 ± 0.8 nm to 21.5 ± 1.0 nm, while the grain size along the growth direction increased by a smaller amount, from 9.2 ± 0.5 nm to 10.3 ± 0.5 nm. (For reference, the Al layer thickness in the as-deposited film was nominally 9.9 nm, comparable to the out-of-plane grain sizes determined from XRD.) To the extent that the Al grain size is proportional to the roughness at the SiC–Al interfaces, the measured increase in grain size upon thermal annealing can partly explain the observed decrease in EUV reflectance with temperature shown in Fig. 5. However, judging from the HRTEM images of Fig. 6, it is doubtful that increased interfacial roughness is the only cause of the measured reflectance decrease upon heating to 300 °C; other mechanisms, e.g., changes in the optical constants of the nominal SiC and/or Al layers as a result of diffusion of atoms across the interfaces, may contribute significantly to the reflectance decrease as well.

More precise EUV reflectance measurements, using synchrotron radiation at the ALS, were obtained from another SiC/Al film having $N = 40$, $d = 15.2$ nm, and $\Gamma = 0.33$, and the results are shown in Fig. 7. The peak reflectance was measured to be 21%, and the measured bandpass was 1.07 nm FWHM. (The difference is well understood between the results of Fig. 7, made using synchrotron radiation at the ALS, and those presented in Figs. 2 and 4, made on nominally identical films using the laser-plasma

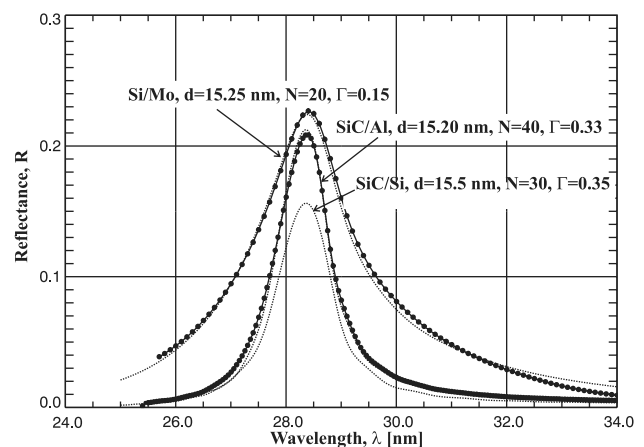


Fig. 7. Reflectance versus wavelength of optimized Si/Mo and SiC/Al multilayers measured using synchrotron radiation at the ALS. The dotted curves are fits to the measurements (filled circles.) Also shown is the calculated response of an optimized SiC/Si multilayer, which provides spectral resolution similar to SiC/Al, but with lower reflection efficiency.

reflectometer at RXO: the difference is due to the greater spectral resolution and signal-to-noise ratio of the ALS reflectometer.) Also shown in Fig. 7 for comparison is the measured reflectance of a Si/Mo multilayer film tuned to the same wavelength and optimized for narrow spectral bandpass ($N = 20$, $d = 15.25$ nm, $\Gamma = d_{\text{Mo}}/d = 0.15$). Fits to the SiC/Al and Si/Mo films are shown in the figure as well (the values of d and Γ noted above were determined from these fits), along with the calculated response of a SiC/Si multilayer optimized for this wavelength. Unfortunately, no experimental data were available for SiC/Si at this wavelength; however, the calculation shown in Fig. 7 is realistic, as it is based on a fit to the measured performance of a similar SiC/Si multilayer that was tuned to $\lambda = 30.4$ nm.

While the Si/Mo multilayer shown in Fig. 7 gives slightly higher reflectance— $R_{\text{max}} = 22.6\%$ —the spectral bandpass is much larger: 1.96 nm FWHM for Si/Mo versus 1.07 nm FWHM for SiC/Al. From the results of Fig. 7 we can see that if such coatings were used for a solar telescope tuned to the Fe XV emission line ($\lambda = 28.4$ nm), the SiC/Al system would provide significantly better rejection of unwanted He II ($\lambda = 30.4$ nm) radiation, with only slightly lower throughput at the target wavelength of 28.4 nm. Specifically, the ratio of the system efficiency at $\lambda = 28.4$ nm ($R_{28.4}$) to the efficiency at $\lambda = 30.4$ nm ($R_{30.4}$) for a two-reflection telescope (e.g., a Cassegrain-type instrument) is $(R_{28.4}/R_{30.4})^2 = 12$ when using Si/Mo multilayer coatings versus $(R_{28.4}/R_{30.4})^2 = 150$ when using SiC/Al multilayers, a 12.5 \times improvement. Furthermore, the as-deposited stress in the SiC/Al coating (-250 MPa) is relatively low, whereas the stress measured in the Si/Mo film is quite high (-1200 MPa), thus necessitating in some cases the use of an adhesion layer of Cr or Ti to reduce the risk of coating adhesion failures or substrate distortions. Because such adhesion layers can have significant roughness, they will reduce the peak reflectance of the Si/Mo coating slightly so, in practice, optimized Si/Mo multilayers with Cr or Ti adhesion layers would provide only a minimal (or no) increase in throughput over SiC/Al multilayers at this wavelength.

As for SiC/Si, we can see from Fig. 7 that SiC/Al provides very similar spectral resolution, but significantly higher peak reflectance. And, as in the case of Si/Mo, SiC/Si multilayers have much higher film stress than SiC/Al, so adhesion layers also would be required for many applications.

The measured reflectance of the SiC/Al multilayer shown in Fig. 7 agrees very well with the theoretical reflectance computed using the optical constants from [19], assuming relatively large interface widths, $\sigma = 2.05$ nm. (For all EUV reflectance fits of as-deposited SiC/Al multilayers, we have also assumed a 1-mm-thick a-SiO₂ top layer, which, based on the temporal stability results described below, we suspect forms on the top SiC layer upon exposure to air.) The large interface widths required for good

agreement with the measurements are consistent with the large interfacial roughness evident in the HRTEM images shown in Fig. 6: ignoring for the moment any issues of HRTEM image artifacts due to sample preparation, finite sample thickness, sample tilt, defocus position, etc., the extent of the interfacial roughness evident in the HRTEM images is approximately 2.5 nm peak-to-valley, which is commensurate with the values derived from fitting the EUV reflectance.

In order to assess the temporal stability of our SiC/Al multilayers we have measured the reflectance versus wavelength of two particular samples over a time span of more than 4 years after deposition. Specifically, we have monitored the reflectance of two SiC/Al films tuned near $\lambda = 19.5$ nm ($d = 10.0$ nm) and 21.1 nm ($d = 10.9$ nm), both having $N = 80$ bilayers. The samples were stored in air. (These films have $\Gamma = 0.5$, and were made without consideration of the optimal layer thickness ratio as discussed above. Consequently, the peak reflectance values reported below are somewhat lower than the reflectance of subsequently made films having $\Gamma = 0.33$ designed for these same wavelengths.)

The peak reflectance of these two films is shown as a function of time in Fig. 8. The as-deposited peak reflectance values were measured to be $R_{\text{max}} = 22.6 \pm 0.25\%$ for the film having $d = 10.0$ nm ($\lambda = 19.5$ nm), and $R_{\text{max}} = 20.5 \pm 0.25\%$ for the $d = 10.9$ nm ($\lambda = 21.1$ nm) film, while the peak reflectances measured after more than 4 years were found to be $R_{\text{max}} = 22.1 \pm 0.25\%$ and $R_{\text{max}} = 19.5 \pm 0.25\%$, respectively. No measurable changes in peak wavelength were observed. In the case of the film having $d = 10.9$ nm, several measurements were made within the first 2 weeks of deposition (shown in the inset), along with a measurement made roughly 8 months after deposition. From these measurements, we see that the peak reflectance of this film evidently drops rapidly during the first 2

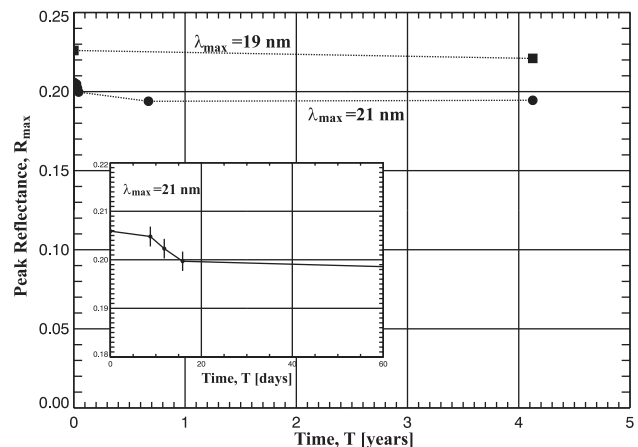


Fig. 8. Peak reflectance measured as a function of time for two SiC/Al multilayers, one peaking near $\lambda = 19$ nm and the other near $\lambda = 21$ nm, as described in the text. The inset shows the behavior in detail of the film that peaks near $\lambda = 21$ nm over the first 60 days of exposure to air.

to 3 weeks of storage. Furthermore, the peak reflectance measured after 8 months was $R_{\max} = 19.5 \pm 0.25\%$, the same (within experimental uncertainty) as that measured after 4 years. These data suggest that the drop in reflectance over time occurs relatively quickly after deposition, presumably as the result of oxidation of the top layer of SiC; indeed, modeling indicates that the measured reflectance drop is consistent with the formation of ~ 1 nm of a-SiO₂ on the surface of the film. In any case, the results shown in Fig. 8 indicate that the EUV performance of these films is quite stable over a period of at least 4 years, and there is no evidence to suggest that further changes in performance will occur over time.

In addition to the SiC/Al multilayer films already discussed, we have made other SiC/Al coatings with periods as large as $d = 50$ nm, in order to ascertain the EUV performance of this multilayer structure over the wavelength range $\lambda = 19$ –80 nm. The films all have $\Gamma = 0.33$, and the number of periods was selected for each sample such that additional periods beyond what was actually deposited would have produced no additional increases in reflectance, based on calculations.

Shown in Fig. 9 are the reflectance-versus-wavelength data obtained on nine such SiC/Al films, with periods spanning the range $d = 10$ –50 nm, as indicated. The results shown in Fig. 9 represent a composite of measurements: the $d = 10$ nm film was measured using the laser-plasma reflectometer at RXO; the films having $d = 15, 16.5$, and 18.5 nm were measured using synchrotron radiation at the ALS; and the films having $d = 20, 27.5, 35, 42.5$, and 50 nm were measured using synchrotron radiation at the NSLS.

Also shown in Fig. 9 are the fits to the measured reflectance curves. We have assumed a 1-mm-thick a-SiO₂ top layer in all cases, based on the temporal stability results described above (these films were all measured several weeks after deposition), and have

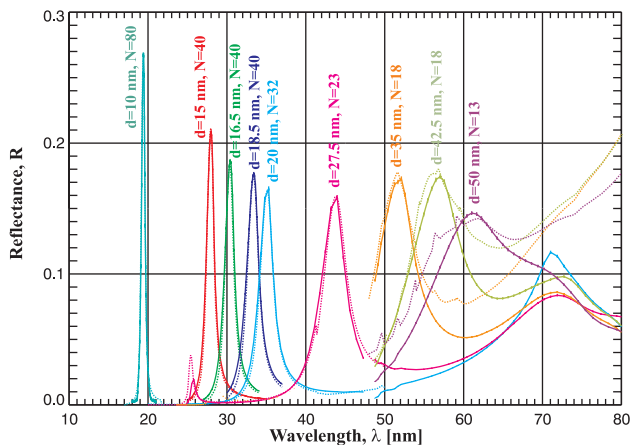


Fig. 9. (Color online) Reflectance versus wavelength measurements (solid curves) obtained on nine different SiC/Al multilayers having the periods and number of bilayers indicated. All films have $\Gamma = 0.33$. The calculated reflectance curves are shown as dotted curves.

used the optical constants for SiC, Al, and a-SiO₂ from [19]. We find good agreement between the measured and calculated reflectance in all cases, although at wavelengths longer than $\lambda \sim 55$ nm, outside of the Bragg peaks, the calculated reflectance begins to deviate significantly from the measurements, predicting somewhat higher reflectance than was measured. Furthermore, the five films measured out to $\lambda = 80$ nm all show a reflectance maximum near $\lambda = 71$ –73 nm, apparently unrelated to the multilayer period. These discrepancies between measurement and calculation could be due, in part, to an imperfect description of the top layer of the films (i.e., 1 nm of a-SiO₂), and possibly due to inaccurate optical constants at these wavelengths as well.

Shown in Fig. 10 are plots of peak reflectance and spectral bandpass (FWHM) as a function of peak wavelength, derived from the results shown in Fig. 9. As is apparent from Figs. 9 and 10, the peak reflectance is highest, and the spectral bandpass lowest, just longward of the Al L-edge near 17 nm. As the multilayer period increases, the peak reflectance decreases and the spectral bandpass increases, for peak wavelengths of up to about $\lambda = 45$ nm. But for the films designed for wavelengths longer than 45 nm, while the spectral bandpass continues to increase, the peak reflectance increases somewhat as well, except for the film that peaks near $\lambda = 61$ nm, which has the lowest reflectance of all, below 15%.

The trends in performance with multilayer period just described are the same as those expected from

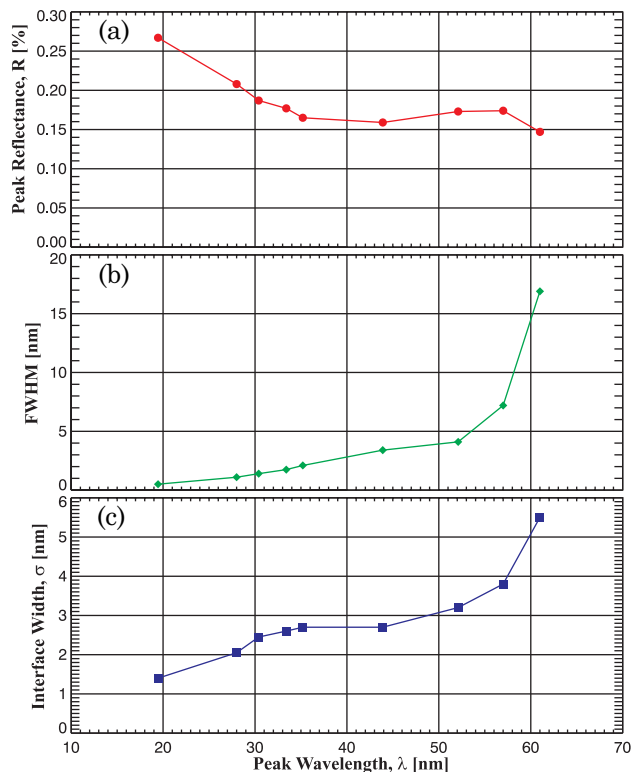


Fig. 10. (Color online) (a) Peak reflectance, (b) spectral bandpass, and (c) interface widths derived from the reflectance measurements for the SiC/Al multilayers shown in Fig. 9.

modeling, although the measured peak reflectance values are consistently lower than those expected theoretically for the case of films having perfectly smooth, sharp interfaces. For example, the maximum theoretical reflectance at $\lambda = 19.5$ nm is 43.8%, as compared to the experimental value of 26.7%, while at $\lambda = 60$ nm, the theoretical maximum is 35.2% versus the experimental value of 14.7%.

Also shown in Fig. 10, as a function of peak wavelength, are the interface widths derived from fits to the reflectance data shown in Fig. 9. While these interface widths have not been determined with perfect accuracy, as is evident from Fig. 9, the values are nevertheless quite large, and increase monotonically with peak reflectance/multilayer period. Based on the HRTEM results of Fig. 6, this increase in interface width with multilayer period is presumably due to interfacial roughness resulting from the Al crystallites that comprise the Al layers: crystallite size typically scales with layer thickness and, in these films, the Al layer thickness increases with multilayer period, so that could explain the trend shown in Fig. 10.

In an effort to produce SiC/Al multilayers having smoother interfaces and, thus, potentially higher EUV reflectance, we have deposited some SiC/Al multilayers using reactive sputtering with a nitrogen–argon gas mixture. In previous studies of other multilayers, such as W/B₄C, we have found that reactive sputtering with N₂ can produce amorphous nitrogen-rich metal layers having greatly reduced roughness (and stress) [20], and so we had hoped that the same effects could be achieved with SiC/Al multilayers. The potential problem in depositing such films by reactive sputtering with N₂ is that the optical properties of the individual SiC and Al layers are likely to change drastically in the EUV, potentially degrading the EUV reflectance of the multilayer and, thus, offsetting any potential gains resulting from smoother interfaces. As will be seen below, that appears to be the case. (For multilayers

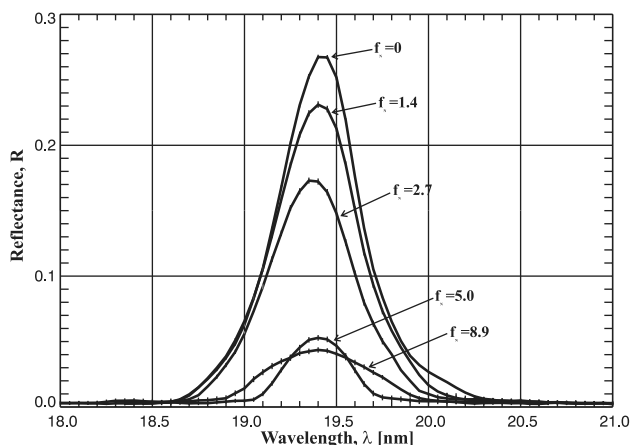


Fig. 11. Reflectance versus wavelength measurements for SiC/Al multilayers deposited using reactive sputtering with nitrogen, having $d \sim 10$ nm, $N = 80$, and $\Gamma = 0.33$, as a function of the N₂ gas fraction, f_N , as described in the text.

designed for shorter wavelengths in the x-ray band this is not a significant problem: the incorporation of a small amount of nitrogen into the film does not strongly affect the x-ray optical properties.)

Shown in Fig. 11 are the reflectance-versus-wavelength measurements made on a series of films (all having $N = 80$, $d = 10$ nm, $\Gamma = 0.33$, thus having peak reflectance near $\lambda = 19.4$ nm), for which we have systematically varied the ratio of N₂ to Ar sputter gas flow during deposition. We quantify the amount of N₂ used in terms of the “N₂ gas fraction,” f_N , which we define as the measured N₂ gas flow rate [i.e., in units of standard cubic centimeters per minute (scm)] divided by the sum of the N₂ gas flow rate plus the Ar gas flow rate. The films shown in Fig. 11 were deposited with f_N in the range of 0% to 9%. In Fig. 12 we plot the peak reflectance as a function of f_N , as determined from the measurements shown in Fig. 11. As is evident from these two figures, the addition of N₂ gas during sputter deposition of SiC/Al multilayers only degrades EUV performance: the peak reflectance falls nearly linearly up to $f_N = 5\%$, and then continues to fall more slowly at larger f_N values. The film made with $f_N = 9\%$ has peak reflectance of only $\sim 4\%$, compared with the $\sim 27\%$ peak reflectance found for the film made with $f_N = 0\%$.

To determine the effect of reactive sputtering with nitrogen on the microstructure of the SiC and Al layers, and on the nature of the SiC–Al interfaces, HRTEM analysis was performed on two of the films shown in Figs. 11 and 12, those having $f_N = 0\%$ and $f_N = 9\%$. Resultant HRTEM images are shown in Fig. 13, along with typical SAED patterns from each film. It is evident from the HRTEM and SAED results of Fig. 13 that reactive sputtering with N₂ does indeed destroy almost completely the crystallinity of the Al layers: while Al lattice fringes predominate in the film deposited using only Ar gas, almost no lattice fringes are evident in the image of the reactively sputtered film. Similarly, well-defined Bragg diffraction spots are almost entirely absent from the SAED pattern obtained with the reactively sputtered film.

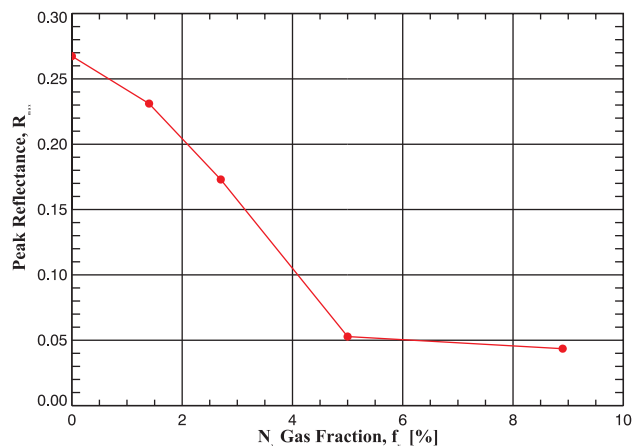


Fig. 12. (Color online) Peak reflectance as a function of N₂ gas fraction, f_N , determined from the measurements shown in Fig. 11.

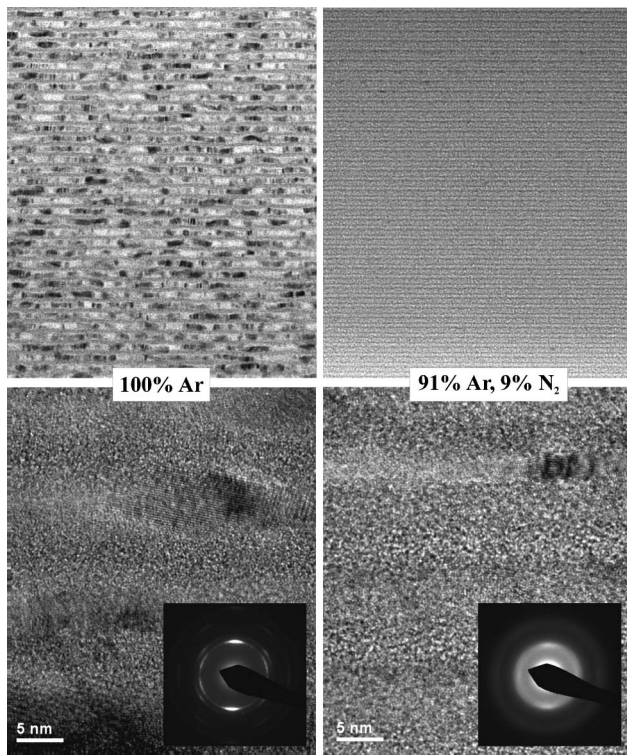


Fig. 13. HRTEM and SAED images for SiC/Al multilayers deposited nonreactively using Ar (left) and reactively using an Ar–N₂ mixture having $f_N = 9\%$.

Also evident from the HRTEM images of Fig. 13 is a large reduction in interfacial roughness, which is probably due to the absence of large Al crystallites in the reactively sputtered film.

Based on the results of Figs. 11–13 just described, we postulate that, although reactive sputtering with nitrogen can result in nearly amorphous Al layers and much reduced interfacial roughness, the incorporation of nitrogen and/or the formation of nitrides in SiC/Al multilayers must cause a large change in optical constants in the individual Al and/or SiC layers such that the EUV reflectance is strongly degraded. While the results obtained here refer to films that peak near $\lambda = 19$ nm, the presumed effect of reactive sputtering with nitrogen on the Al and/or SiC optical constants will likely be even more problematic at longer EUV wavelengths, where the absorption in these layers is already significantly higher than at $\lambda = 19$ nm.

4. Summary and Conclusions

We have studied the performance, structure, and stability of periodic SiC/Al multilayer films designed as normal-incidence reflectors for use at EUV wavelengths below the Al L-edge near $\lambda = 17$ nm. For structures having a fractional SiC layer thickness of $\Gamma_{\text{SiC}} = 0.33$, and with periods in the range of $d = 10$ – 50 nm (i.e., such that the peak reflectance occurred at wavelengths spanning the range of $\lambda \sim 19$ – 62 nm), we find peak reflectance values in the range $R_{\text{max}} = 15$ – 27% , depending on wavelength,

with the highest reflectance occurring at the shortest wavelengths, i.e., those closest to the Al L-edge. While the spectral bandpass of these coatings increases with multilayer period, as expected, it is nevertheless much smaller than many other multilayer material combinations (such as Si/Mo and others) that work well at these same wavelengths, particularly over the wavelength range of $\lambda = 17$ – 35 nm. These multilayers have relatively small compressive film stresses, and reflectance measurements made over a period of more than 4 years indicate excellent temporal stability.

From HRTEM analysis of SiC/Al multilayers we find that the SiC layers are amorphous and the Al layers polycrystalline with a strong (111) texture. The Al crystallites apparently give rise to relatively large roughness at the SiC–Al interfaces. Fits to the EUV data also suggest large interface widths, commensurate with the HRTEM data, and the interface width increases with multilayer period. It is likely, therefore, that significantly higher EUV reflectance could be achieved if the interfacial roughness could somehow be reduced.

The large interface widths we find are comparable to the interface widths determined from XRR in SiC/Al multilayers reported by Jonnard *et al.* [13]. Using a variety of characterization techniques complementary to those used here, namely x-ray emission spectroscopy and time-of-flight secondary ion mass spectroscopy, they conclude that the interface widths in their multilayers are primarily the result of interfacial roughness, rather than interfacial diffusion, just as we observe from HRTEM analysis. Those authors also explored the use of Mo and W barrier layers in their multilayers, with the goal of reducing interfacial roughness. From XRR measurements, they find a dramatic reduction in interfacial roughness, from $\sigma = 2.8$ nm to $\sigma = 1$ nm or less, when such refractory metals are used as barrier layers. No normal-incidence reflectance measurements of their films were reported, however, so it will be interesting to see if the EUV performance of the films containing refractory metal barrier layers is indeed better than films deposited without barrier layers. Also, Jonnard *et al.* used an alloy of Al containing 1% Si, rather than pure Al, as was used here, which they suggest results in smoother Al layers; it will thus be interesting to compare the EUV performance of SiC/AlSi versus SiC/Al multilayers as well.

Our efforts to improve the EUV performance in SiC/Al multilayers by depositing these films using reactive sputtering with nitrogen were unsuccessful. While HRTEM measurements of reactively sputtered SiC/Al multilayers show nearly amorphous Al layers with greatly reduced interfacial roughness, the EUV performance of these films was nevertheless poor. We suspect that the low reflectance in reactively sputtered films is due to changes in the optical constants of the individual Al and/or SiC layers as a result of nitrogen incorporation and/or nitride formation.

In conclusion, we have demonstrated that SiC/Al multilayers can provide good performance in the EUV, especially for applications requiring a narrow spectral bandpass. For the wavelength range of $\lambda \sim 25\text{--}35\text{ nm}$ in particular, SiC/Al provides higher reflectance than SiC/Si multilayers, and much better spectral resolution than Si/Mo, SiB₄C, and SiC/Mg multilayers. This stable, low-stress coating thus represents an attractive option for applications that require good spectral selectivity, such as narrow-band solar imaging. For example, a two-reflection solar telescope tuned to the Fe XV emission line at $\lambda = 28.4\text{ nm}$ coated with SiC/Al multilayers would provide 12.5 times greater rejection of unwanted He II ($\lambda = 30.4\text{ nm}$) radiation relative to a telescope coated with optimized Si/Mo multilayers, while providing approximately the same efficiency at the target wavelength.

The authors would like to acknowledge the essential contributions of B. Kjornrattanawanich, J. F. Seely, and E. M. Gullikson, who performed the EUV reflectometry measurements using synchrotron radiation reported here. This research was sponsored in part by contract number 8100001371 from Lockheed-Martin Corporation.

References

- J. P. Delaboudinière, G. E. Artzner, J. Brunaud, A. H. Gabriel, J. F. Hochdeh, F. Millier, X. Y. Song, B. Au, K. P. Dere, R. A. Howard, R. Kreplin, D. J. Michels, J. D. Moses, J. M. Defise, C. Jamar, P. Rochus, J. P. Chauvineau, J. P. Marioge, R. C. Catura, J. R. Lemen, L. Shing, R. A. Stern, J. B. Gurman, W. M. Neupert, A. Maucherat, F. Clette, P. Cugnon, and E. L. Van Dessel, "EIT: extreme-ultraviolet imaging telescope for the SOHO mission," *Sol. Phys.* **162**, 291–312 (1995).
- J. F. Seely, C. M. Brown, D. L. Windt, S. Donguy, and B. Kjornrattanawanich, "Normal-incidence efficiencies of multilayer-coated laminar gratings for the extreme-ultraviolet imaging spectrometer on the Solar-B mission," *Appl. Opt.* **43**, 1463–1471 (2004).
- R. Soufli, D. L. Windt, J. C. Robinson, E. Spiller, F. J. Dollar, A. L. Aquila, E. M. Gullikson, B. Kjornrattanawanich, J. F. Seely, and L. Golub, "Development and testing of EUV multilayer coatings for the atmospheric imaging assembly instrument aboard the Solar Dynamics Observatory," *Proc. SPIE* **5901**, 59010M (2005).
- I. Yoshikawa, T. Murachi, H. Takenaka, and S. Ichimaru, "Multilayer coating for 30.4 nm," *Rev. Sci. Instrum.* **76**, 066109 (2005).
- J. M. Slaughter, B. S. Medower, R. N. Watts, C. Tarrío, T. B. Lucatorto, and C. M. Falco, "Si/B₄C narrow-bandpass mirrors for the extreme ultraviolet," *Opt. Lett.* **19**, 1786–1788 (1994).
- D. L. Windt, S. Donguy, J. F. Seely, B. Kjornrattanawanich, "Experimental comparison of extreme-ultraviolet multilayers for solar physics," *Appl. Opt.* **43**, 1835–1848 (2004).
- Yu. A. Uspenskii, V. E. Levashov, A. V. Vinogradov, A. I. Fedorenko, V. V. Kondratenko, Yu. P. Pershin, E. N. Zubarev, and V. Yu. Fedotov, "High-reflectivity multilayer mirrors for a vacuum-ultraviolet interval of 35–50 nm," *Opt. Lett.* **23**, 771–773 (1998).
- B. Kjornrattanawanich, D. L. Windt, and J. F. Seely, "Normal-incidence silicon-gadolinium multilayers for imaging at 63 nm wavelength," *Opt. Lett.* **33**, 965–967 (2008).
- M. Fernández-Perea, M. Vidal-Dasilva, J. I. Larruquert, J. A. Méndez, and J. A. Aznárez, "Narrowband filters and broadband mirrors for the spectral range from 50 to 200 nm," *Proc. SPIE* **7018**, 70182W (2008).
- Unpublished results for Al/Zr multilayers by F. Salmassi and E. M. Gullikson, and by J. Kortright, as listed at <http://henke.lbl.gov/cgi-bin/mldata.pl>
- D. L. Windt, unpublished.
- T. Sakao, S. Tsuneta, H. Hara, R. Kano, T. Yoshida, S. Nagata, T. Shimizu, T. Kosugi, K. Murakami, W. Wasa, M. Inoue, K. Miura, K. Taguchi, and K. Tanimoto, "Japanese sounding rocket experiment with the solar XUV Doppler telescope," *Proc. SPIE* **2804**, 153–164 (1996).
- P. Jonnard, K. Le Guen, M.-H. Hu, J.-M. André, E. Meltchakov, C. Hecquet, F. Delmotte, and A. Galtayries, "Optical, chemical and depth characterization of Al/SiC periodic multilayers," *Proc. SPIE* **7360**, 73600O (2009).
- X. Deng, C. Cleveland, T. Karcher, M. Koopman, N. Chawla, and K. K. Chawla, "Nanoindentation behavior of nanolayered metal-ceramic composites," *J. Mater. Eng. Perform.* **14**, 417–423 (2005).
- D. L. Windt and W. K. Waskiewicz, "Multilayer facilities required for extreme-ultraviolet lithography," *J. Vac. Sci. Technol. B* **12**, 3826–3832 (1994).
- D. L. Windt, "IMD—Software for modeling the optical properties of multilayer films," *Comput. Phys.* **12**, 360–370 (1998).
- G. G. Stoney, "The tension of metallic films deposited by electrolysis," *Proc. R. Soc. London A* **82**, 172–175 (1909).
- J. H. Underwood, E. M. Gullikson, M. Koike, P. J. Batson, P. E. Denham, K. D. Franck, R. E. Tackaberry, and W. F. Steele, "Calibration and standards beamline 6.3.2 at the Advanced Light Source," *Rev. Sci. Instrum.* **67**, 3372 (1996).
- Handbook of Optical Constants of Solids*, E. D. Palik, ed. (Academic, 1985).
- D. Windt, "Reduction of stress and roughness by reactive sputtering in W/B₄C multilayer films," *Proc. SPIE* **6688**, 66880R (2007).